



Four decades of winter wetland changes in Poyang Lake based on Landsat observations between 1973 and 2013



Xingxing Han, Xiaoling Chen, Lian Feng

State Key Laboratory of Information Engineering in Surveying, Mapping and Remote Sensing, Wuhan University, Wuhan 430079, China

ARTICLE INFO

Article history:

Received 21 July 2014

Received in revised form 26 September 2014

Accepted 7 October 2014

Available online 6 November 2014

Keywords:

Poyang Lake

Wetland

Remote sensing

SVM classification

Landsat

Empirical line correction

Atmospheric correction

ABSTRACT

Poyang Lake, the largest freshwater lake of China, is well known for its ecological importance as a dynamic wetland system. However, due to the significant seasonality of the lake's inundation area, no systematic study has assessed the wetland changes over the past few decades. We addressed this challenge by using four decades of Landsat observations ranging from 1973 to 2013. The images were acquired in the same season to ensure similar phenological and hydrological conditions during each year. Extensive training and validation samples were collected from high-resolution Quickbird imagery to develop a Support Vector Machines (SVM) method for wetland classification of Poyang Lake. To obtain consistent results from different Landsat instruments, an empirical line correction approach was introduced to adjust the sensor-associated differences in band configurations and spectral responses. Significant changes in the major wetland cover types in Poyang Lake were revealed from long-term classification maps. The vegetation coverage of Poyang wetland showed a statistically significant increasing trend during the overall period ($15.9 \text{ km}^2 \text{ year}^{-1}$), and the vegetation tended to spread into the lake center in the Nanjishan Wetland National Nature Reserve (NWNNR) in recent years. At the same time, out-of-phase variability was observed for the mudflats since 1984, with a significant shrinking trend of $-12.1 \text{ km}^2 \text{ year}^{-1}$ ($p < 0.05$). Although sand coverage experienced a rapid decrease from 1973 to 1990 (from 544.3 km^2 to 62.9 km^2), it remained at a relative stable low level ($<100 \text{ km}^2$) in the following period. The two national reserves in Poyang Lake shared change patterns similar to those of the entire lake. Although $\sim 70\%$ of the long-term changes in the wetland vegetation area appeared to be explained by local temperature, there was rapid increase after 2002 possibly due to the impoundment of the Three Gorges Dam (TGD) in 2003. The large sand area in 1973 was potentially linked to previous human activities in China between the 1950s and the 1970s. The method used in this study could be easily extended to other places in the world to assess the decadal wetland changes, and the information provided in this work is critical for future restoration efforts of the Poyang Lake wetland ecosystem.

© 2014 Elsevier Inc. All rights reserved.

1. Introduction

Wetland systems at the land–water interface often provide critical ecosystem functions, i.e., flood reduction, fish production, carbon storage, conservation of biological diversity, etc. (Gibbs, 2000; Houlahan, Keddy, Makkay, & Findlay, 2006; Keddy, 2010; Mitsch & Gosselink, 2000). However, due to intensive human activities and species invasions, dramatic changes in the wetland landscape have occurred worldwide over recent decades (Gibbs, 2000; Gong et al., 2010), degrading their ecological functions and triggering numerous environmental and social problems. Thus, accurate monitoring and understanding of wetland changes are of significant importance to both the scientific community and local governments.

Assessments of large wetlands are often challenging because the distribution and composition of different wetland cover types are

heterogeneous across space and time (Houlahan et al., 2006). Additionally, phenological cycles of different wetland vegetation species require frequent observations within their growth seasons. Thus, traditional measurements, i.e. field surveys or gauge stations, are limited by either spatial or temporal coverage. With its advantages of synoptic and repeated observations, remote sensing has become one of the most efficient methods in wetland monitoring (Adam, Mutanga, & Rugege, 2010). Remote sensing not only can provide frequently wetland maps but also yields information on surrounding land uses and their changes over time, information that could potentially be used to understand the wetland changes (Ozesmi & Bauer, 2002).

Various methods have been developed to discriminate and map wetland cover types using multi-spectral and hyperspectral images. Early work with satellite data used visual interpretation to identify wetlands through true color or false color composites (Best & Moore, 1979; Johnston & Barson, 1993). Currently, computerized methods (i.e., unsupervised/supervised classification, principal component analysis and hybrid classification) are used to identify and classify wetland

E-mail address: lian.feng@whu.edu.cn (L. Feng).

habitat types according to different application requirements and data sources (Franklin, Gillespie, Titus, & Pike, 1994; Gluck, Rempel, & Uhlig, 1996; Hines, Peltier, & Crill, 1984–2012; Hinson, German, & Pulich, 1994; Kempka, Kollasch, & Koeln, 1992; Lee & Marsh, 1995; Luczkovich, Wagner, Michalek, & Stoffle, 1993; Macleod & Congalton, 1998; Margono, Bwangoy, Potapov, & Hansen, 2014). Certain studies also attempted to estimate the biophysical and biochemical properties of wetland vegetation using remotely sensed imagery (Proisy, Couteron, & Fromard, 2007; Green, Mumby, Edwards, Clark and Ellis, 1997; Kovacs, Flores-Verdugo, Wang, & Aspden, 2004; Kovacs, Wang, & Flores-Verdugo, 2005), where *in situ* measurements were used to calibrate and validate the retrieval models.

Poyang Lake is the largest freshwater lake of China, and its exposed flood plain in the dry seasons is one of the most important wetlands in the world, as recognized by the International Union for the Conservation of Nature (Finlayson, Harris, McCartney, Lew, & Zhang, 2010). The Poyang Lake wetland serves as the largest winter habitat for over 90% of Siberian migratory birds, and regions covered by *Carex cinerascens* (one typical wetland plant in the lake) provide unique spawning beds and feeding grounds for local fish (Zhang, 1988). However, in recent years, the Poyang wetland was reported to be destroyed due to enhanced human activities, i.e., poplar planting and reclamation in the emerged floodplains (Li, 2008). In addition, illegal sand dredging has led to increased turbidity of the lake water (Feng, Hu, Chen, Cai, et al., 2012), inhibiting the productivity of submerged vegetation and thus threatening the habitat for migrating birds in winter (Wu, Leeuw, Skidmore, Prins, & Liu, 2005).

Several pioneering researchers have attempted to study the Poyang Lake wetland using remote sensing approaches. For example, multispectral images collected during different seasons of a year were used to discriminate wetland vegetation of different species and functional types (Wang et al., 2012). Object-based image analysis was applied by Dronova, Gong, and Wang (2011, 2012) to obtain high accuracy in classifications of the functional types of wetland plants of the lake. Using Landsat ETM+ images and field biomass data, Tan, Shao, Yang, and Wei (2003) also attempted to establish a model for estimating the wetland vegetation biomass in Poyang Lake.

However, due to the significant seasonality of the lake's inundation area (Feng, Hu, Chen, Cai, et al., 2012), it is difficult to compare the classified wetland maps of Poyang Lake between different years. Thus, to date, no systematic assessment of the long-term changes in Poyang Lake's wetland has been accomplished, not to mention the potential linkage with natural processes and/or anthropogenic activities. In this study, we addressed the technical challenges using Landsat measurements in the dry seasons over a four-decade period (1973–2013) with the following two objectives:

- (1) Develop a reliable method to classify the major wetland cover types of Poyang Lake using Landsat images, which overcomes the difficulties of sensor associated-differences and atmospheric correction.
- (2) Document the long-term changes of different wetland features over the last four decades in Poyang Lake and understand their relationships to climate variability and human activities.

2. Study area and dataset

2.1. Study area and environmental settings

Poyang Lake is located in the north of Jiangxi Province ($28^{\circ}22'$ – $29^{\circ}45'N$ and $11^{\circ}47'$ – $116^{\circ}45'E$, Fig. 1). The lake receives water from precipitation over the lake and inflow from local rivers (Ganjiang River, Fuhe River, Xiushui River, Xinjiang River, and Raohe River). Typically, the lake flows from south to north, and discharges to the Yangtze River at Hukou in the north. When the water level of Yangtze River increases during summer (Shankman, Keim, & Song, 2006), river-lake

flow reversal can also occur. Subtropical monsoons in the local regions lead to great seasonality in precipitation. During the wet seasons from April to September, almost all of the sub-lakes of Poyang Lake are connected to form a large lake, and the inundation area can cover $>3000 \text{ km}^2$ (Feng, Hu, Chen, Cai, et al., 2012). During the dry seasons from October to March, the lake is divided into many connected and disconnected segments separated by the exposed floodplains with a small inundation area of $<1000 \text{ km}^2$.

The emerged lake bottom in the low-water stages serves as the habitat for most of the Serbian migrating cranes and storks (Kanai et al., 2002), making Poyang Lake one of the most renowned wetlands in the world (Finlayson et al., 2010). To conserve rare and endangered migratory birds and the wetland ecosystem of Poyang Lake, the Chinese government has constructed two national nature reserves in the lake area, the Poyang Lake National Nature Reserve (denote as PLNNR in this study) and Poyang Lake Nanjishan Wetland National Nature Reserve (denote as NWNNR; see locations in Fig. 1). Established in 1983 with an area of 224 km^2 , the PLNNR is one of the first six important wetlands that joined the Ramsar Convention (the Convention on Wetlands of International Importance) in China. The NWNNR ($\sim 333 \text{ km}^2$) is located in the mouth of Gan River (the largest tributary of Poyang Lake), which is considered one of the best-conserved wetlands at similar latitudes.

Furthermore, the Poyang Lake boundary used in this study is the same as that reported in Feng, Hu, Chen, Cai, et al., 2012, which was generated based on the large inundation in the wet season.

2.2. Datasets

Two types of data were used in this study: satellite images and gauged hydrological and meteorological measurements.

The satellite data consist of multispectral images collected by Landsat instruments, including MSS, TM, ETM+, and OLI. Geometrically corrected Level 1T (L1T) data were downloaded from United States Geological Survey (USGS) (<http://www.usgs.gov/>) and the Remote Sensing Data Sharing Center of China (<http://ids.ceode.ac.cn/>). Cloud-free images over 40 years were selected through visual examination, and the temporal distribution of the data is listed in Table 1. The satellite images were collected between December and January of the following year, assuring similar environmental and hydrological conditions during each year. Note that the year used in this study is the hydrological year starting on April 1 of the current year and ending on March 31 of the following year because the month of April is the dry-wet transition month.

Air temperature and precipitation data were acquired from the nearest meteorological station of Poyang Lake (Boyang station, see Fig. 1), and were obtained from the China Meteorological Data Sharing Service System (<http://cdc.cma.gov.cn/>). Water level data used in this study were measured at Xingzi station (see location in Fig. 1) and represent the water level of the entire Poyang Lake. Sediment flux data for local tributaries between 1990 and 2010 were obtained from Jiangxi Provincial Institute of Water Sciences to understand its potential influence on the growth of the wetland vegetation.

3. Methodology

3.1. Data pre-processing and reference data selection

Landsat images were firstly converted to top-of-atmosphere (TOA) radiance using radiometric calibration coefficients in the metadata file. Next, the calibrated radiance was processed with the FLAASH module embedded in ENVI 4.8 software, resulting in atmospherically corrected surface reflectance. Incorporated in the FLAASH module is the MODTRAN4 radiation transfer code, which is considered to be a good solution for atmospheric correction in terrestrial applications (Kaufman et al., 1997). The key parameters used in the FLAASH module

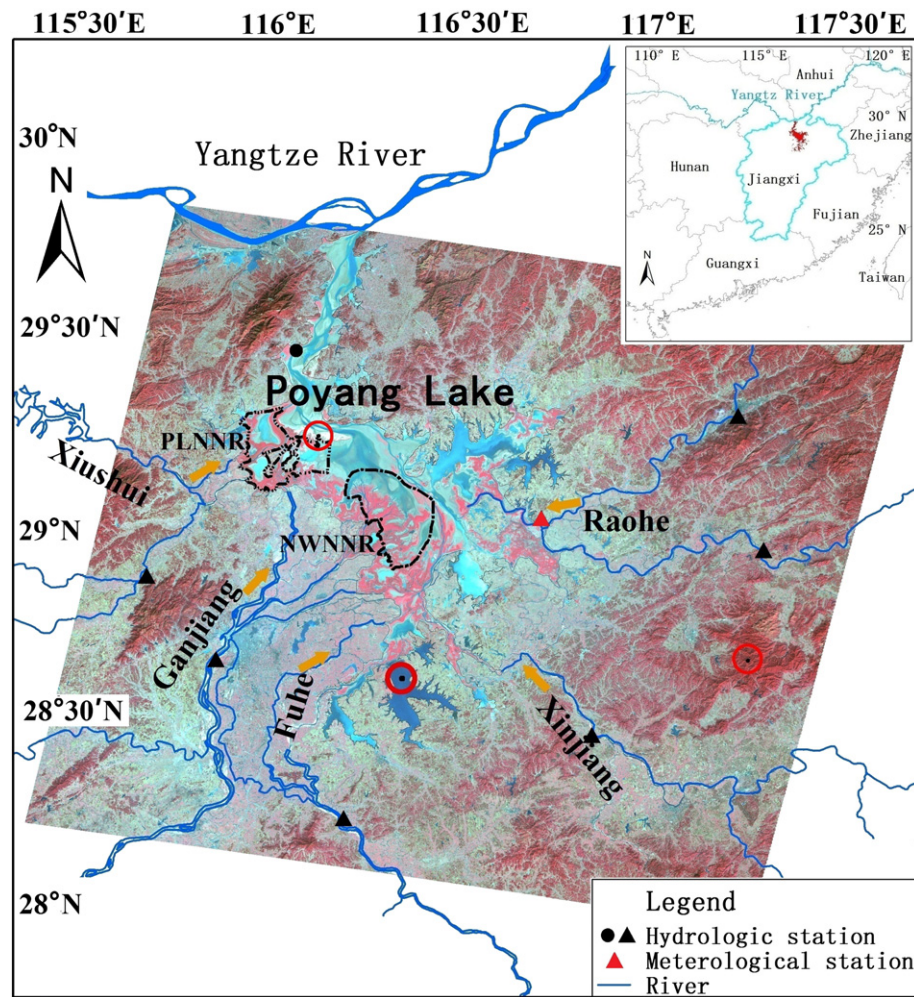


Fig. 1. Location of the Poyang Lake wetland in China. The false color image is the Landsat-8 OLI image collected on December 24, 2013. The boundaries of two national reserves (PLNNR and NWNNR) of Poyang Lake are delineated with black lines. The red-encircled regions are the locations where surface features were relatively stable in the four-decade Landsat observation period. The inset figure shows the location of the lake drainage basin.

are selected as follows: Mid-Latitude Winter for atmospheric model, Rural for aerosol model (because the study area is located far away from urban or industrial sources), and 2-Band (K-T) for the aerosol retrieval; the initial visibility was chosen as 20–40 km depending on the

image quality, and no water retrieval was conducted because no specific band was configured with the Landsat instruments. To match the spatial resolution of the other three Landsat instruments, two MSS images were re-sampled to 30 m using the nearest neighbor resampling method.

The first task of this study is to discriminate the different wetland cover types using Landsat images. Four major wetland cover types exist in Poyang Lake, i.e., water, vegetation, mudflat and sand, and the detailed functions of the four types are listed in Dronova et al. (2011). The frequently used method is supervised classification in which training and validation samples (referred to herein as ‘reference data’) are obtained to develop a robust classifier. Then, the first step selects appropriate training samples, which are representative for the four classes. Ideally, the reference data should be obtained through field surveys; however, the rapid inundation changes and relatively shallow water in the wetland make it difficult to conduct effective field observations in Poyang Lake. Fortunately, high-resolution images are accessible freely from Google Earth™ (<http://earth.google.com>) and could be used as ground-truth for land cover classifications (Knorn et al., 2009). Indeed, four Quickbird images acquired only 3 days before the acquisition date of the Landsat OLI image in 2013 are available in Google Earth in which different wetland cover types could easily be visually interpreted in Poyang Lake (see Fig. 2). Thus, samples selected from the quasi-synchronous Quickbird images were considered as the reference data for classification in this study.

Table 1

Landsat images used in this study. Note that the column ‘year’ indicates the hydrological year of Poyang Lake, starting on April 1 of the current year and ending on March 31 of the next year.

Year	Date	Sensor	Resolution (m)
1973	24/12/1973	MSS	60
1984	8/12/1984	MSS	60
1990*	9/12/1990	TM	30
1995	7/12/1995	TM	30
1996	9/12/1996	TM	30
1999	10/12/1999	ETM +	30
2001	8/1/2002	TM	30
2006*	6/1/2007	TM	30
2008	11/1/2009	TM	30
2009	14/1/2010	TM	30
2013	24/12/2013	OLI	30

* The asterisked files were downloaded from the Remote Sensing Data Sharing Center of China (<http://ids.ceode.ac.cn/>), the other images were obtained from the USGS. Also note that the real resolution of MSS is 78 m, which has been re-sampled to 60 m by the data provider.

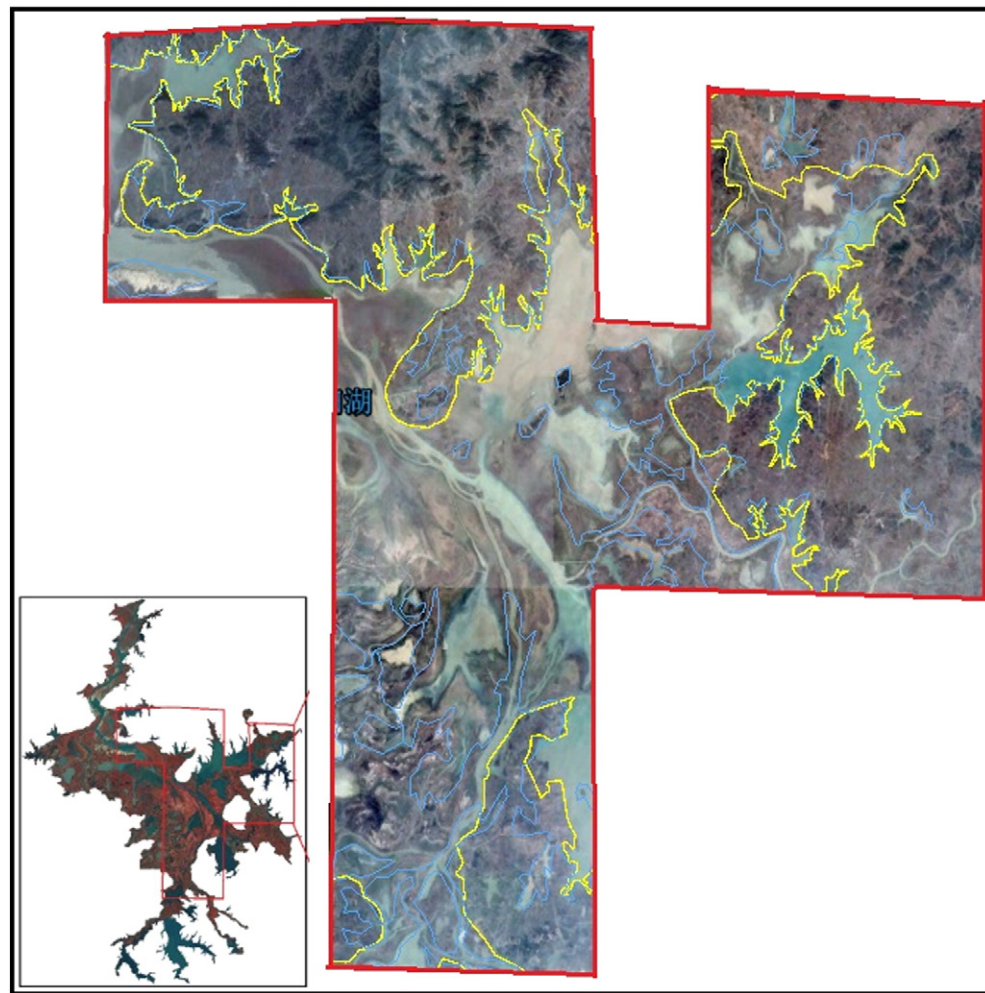


Fig. 2. High-resolution Quickbird images available in Google Earth™ acquired only 3 days before the acquisition date of the Landsat OLI image in 2013. The near concurrent Quickbird images could be used as ground-truth data for wetland classification using the 30-m resolution Landsat OLI imagery.

More than 4000 random points were generated within the overlapped region between the Quickbird and Landsat OLI images (see Fig. 2). Points were visually classified as sand, vegetation, mudflat, and water; of the >400 random points for each class, half of them were used for training and the other half were used for validation. All of the samples were also cross-checked using NDVI (a higher NDVI indicates the higher probability of vegetation) and NDWI (a higher NDWI suggests the higher probability of water), which were calculated with the surface reflectance of Landsat OLI images to avoid the inundation changes of Poyang Lake that occurred between the acquisition dates of the Landsat and Quickbird images (3 days apart). For example, if a high NDWI is obtained for a vegetation point, it is likely that the point has been transitioned into water within the 3-day difference of the acquisition dates and should be excluded from the vegetation samples. Likewise, if a high NDVI is found for a water point, it could have changed into other cover types and should be removed for further analysis.

The means and standard deviations of the Landsat OLI spectrum for the training samples were estimated and plotted in Fig. 3, which clearly reveals that the four wetland cover types are spectrally distinguishable in the visible-to-NIR regions. Indeed, according to sensitivity analysis with additional random points generated for each class (600 and 800 points), the changes in the mean spectra are negligible (<2%), suggesting that the selected training samples could adequately represent the spectral features for each class. Thus, a valid classifier could be expected from those carefully selected samples.

3.2. Image classification

Four typical supervised classification methods were compared in this study to find the best approach for wetland cover type classification

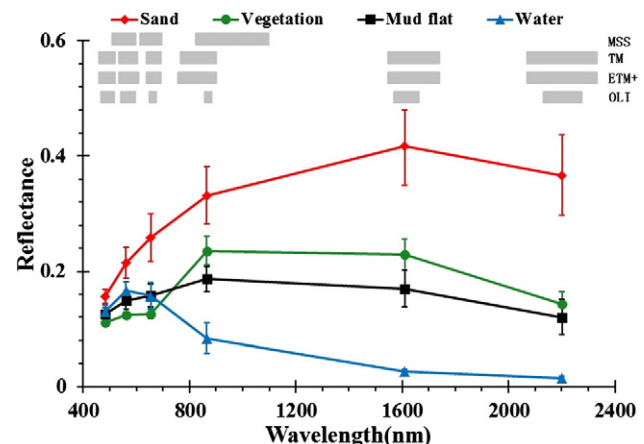


Fig. 3. Mean spectral shape of the selected training samples on the atmospherically corrected OLI images for different wetland classes of Poyang Lake. The standard deviations were also plotted. The gray bars indicate the spectral range of different Landsat instruments. The spectral features of the four classes are highly distinguishable between the visible and NIR regions.

of Poyang Lake, i.e., Support Vector Machines (SVM), Minimum Distance, Mahalanobis Distance and Maximum Likelihood methods (Jensen, 1996). The selected training samples (e.g., surface reflectance of six OLI bands and visually classified cover types from near concurrent Quickbird images) were used to train the classifier for the different methods, and the accuracy measures were estimated using the validation samples (see Table 2). The results show that the SVM method achieved much better performance than the other methods because it demonstrated higher overall accuracy, producer accuracy and kappa coefficient values (Congalton, 1992). With an overall accuracy of over 91% for any given class, the SVM was selected as the candidate approach for classifying the Poyang Lake wetland.

Unfortunately, the Landsat data used in this study were acquired from four different instruments (see Table 1), and the classifier established for OLI may not be suitable for the others due to their varied band configurations and spectral responses (Chander, Markham, & Helder, 2009). As shown in Fig. 3 (gray bars), large discrepancies exist between the band wavelength of OLI and that of the other three sensors. Although TM/ETM + contains spectral bands similar to OLI, the differences in bandwidth are also prominent. Moreover, although MSS has four spectral bands in the visible-to-NIR region, only three analogues of these are shared with OLI (see Table 1).

An ideal solution is to develop image-specific classifiers for each of the selected Landsat image (Knorn et al., 2009); however, it is impossible to obtain concurrent reference data for images acquired several decades ago (i.e., the MSS data). A compromise method in this study uses the OLI-based classifier for all of the Landsat images, and the sensor-associated differences (wavelengths, spectral responses, illuminations, etc.) between OLI and other instruments were corrected. An empirical line method (Smith & Milton, 1999) was introduced to adjust the differences between the atmospherically corrected surface reflectance of OLI and the other instruments (eg. MSS, TM and ETM +). The fundamental concept is that by considering the similarity in acquisition time (December to January of each year in this study), the changes in surface conditions and reflectance among different images should be small if the target is relatively stable. In practice, three targets from sand, clear water and dense forest were first selected in the Landsat images (red-encircled in Fig. 1) in locations where the surface features could be treated as unchanged across the 40-year Landsat observation period. In brief, sand and clear water were easily interpreted through the RGB composites of Landsat images, whereas dense forest was determined through a vigorous comparison of RGB images and spectral features between different Landsat images. To eliminate potential speckle noise or atmospheric failures, the mean reflectance of a small window (5×5 , approximately 150×150 m) centered at these targets was estimated for different spectral bands of the 11 Landsat images.

Using the surface reflectance of the OLI image in 2013 as a reference, the linear relationship between OLI and the other Landsat images (L_x) could be established. The relationship for each band was determined using four points, including the OLI- L_x reflectance pairs from three stable targets and the zero reflectance. The zero reflectance assumed that if the surface reflectance of OLI is zero, the corresponding signal for other instruments also should be zero. Fig. 4 shows a typical example of the empirical relationships between the analogous spectral bands of OLI and TM images, which were acquired in 2013 and 2007,

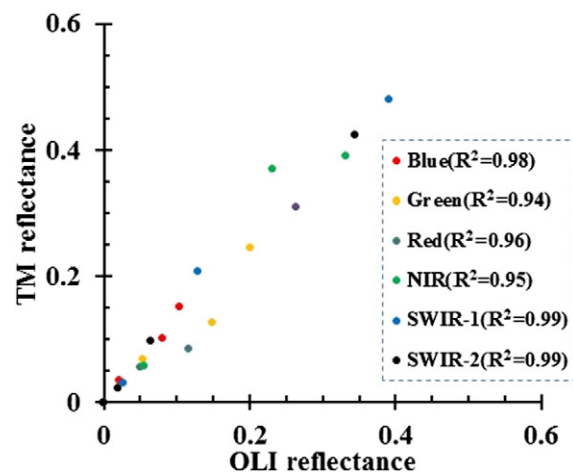


Fig. 4. Relationships between atmospherically corrected OLI (2013) and TM (2007) reflectance for the analogue spectral bands over three stable locations. The zero reflectance was also included to establish the relationship for each band. Tight correlations are clearly observed between all of the analogue bands.

respectively. The TM reflectances appear to have a linear response to the OLI reflectance across a wide range (0–0.5). With $R^2 > 0.94$ for any given bands, the TM reflectance could be adjusted to OLI using a simple linear conversion. Indeed, high correlations ($R^2 > 0.9$) could be observed between other images and the OLI data (see Table 3). Thus, the method was repeated for each band of the other images (six bands for TM/ETM + and three bands for MSS; see Fig. 3), with the surface reflectance of all Landsat images adjusted to the same level as the OLI data in 2013.

For images collected by Landsat MSS, the limited spectral information (three bands analogous to OLI) might not be able to classify the major wetland cover types in Poyang Lake. To verify whether the three visible-to-NIR bands are sufficient for wetland classification, a new SVM classifier was developed with the same training samples as the six-band method, whereas only three OLI bands (analogous to MSS) were used. The accuracy was also estimated using the same validation samples, as tabulated in [Table 2](#). Although only three spectral bands of the OLI image were used, the classified result was similar to the six-band SVM approach. The four wetland cover types show similar spatial distributions between the three- and six-band SVM classification methods (see [Fig. 5](#)), and the accuracy measures for the two methods were almost identical with a difference in overall accuracy of <1.5% (see [Table 2](#)). Therefore, if the sensor-associated differences between MSS and OLI were adjusted (see method described above), valid and consistent classification results could be expected using MSS and the three-band SVM classifier.

To quantify the wetland changes of Poyang Lake during the last four decades, the areas of the major cover types were calculated for each Landsat classification map. The changes in water area were not considered because the differences across each panel may be to the significant inundation seasonality in Poyang Lake (Feng, Hu, Chen, Cai, et al., 2012). Thus, the maximum water area was masked before the areas of the other three cover types were estimated. The water mask was determined as the set of the classified water areas for the 11 Landsat images,

Table 2
Classification accuracy of the different classification methods.

Producers accuracy	SVM_6bands	SVM_3bands	Min_Dis	Max_Like	Maha_Dis
Sand	91.18%	93.55%	96.43%	87.50%	96.30%
Vegetation	96.63%	94.31%	87.10%	93.97%	87.56%
Mudflat	93.88%	90.82%	57.14%	75.00%	49.69%
Water	98.78%	98.78%	88.11%	98.04%	99.20%
Over all	96.43%	95.04%	81.75%	90.28%	78.97%
Kappa	0.95	0.93	0.73	0.86	0.7

Table 3
Correlations (R^2) between analogous spectral bands of OLI in 2013 and the other Landsat images.

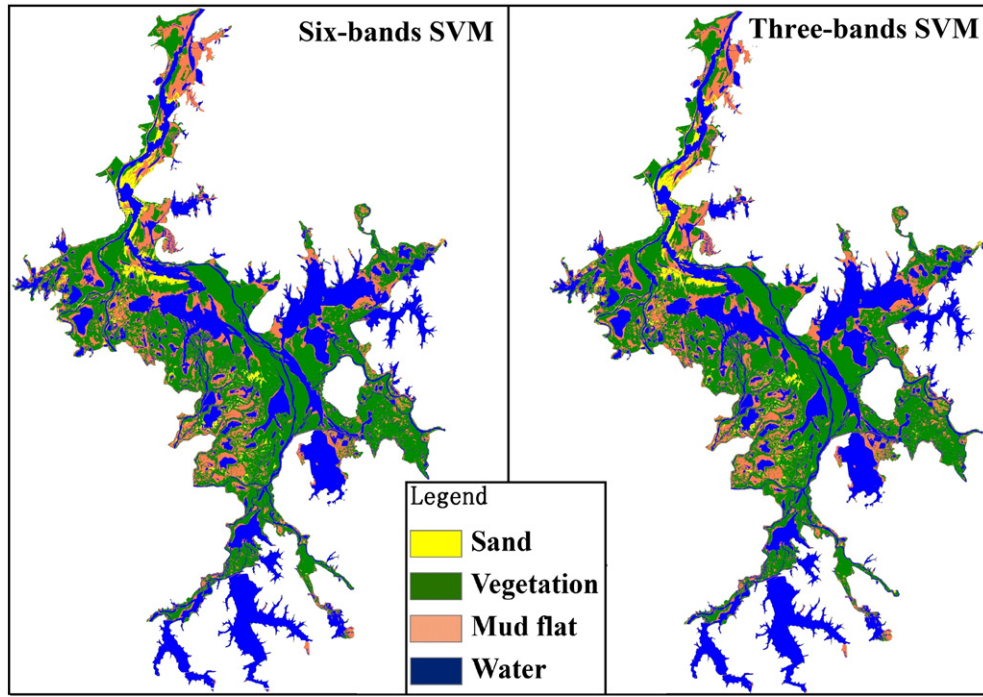


Fig. 5. Comparison between the classification maps of the six-band and three-band SVM methods. The classified wetland maps show nearly identical spatial distributions, indicating that information provided with three spectral bands over the visible to NIR regions is sufficient to classify the wetland cover types in Poyang Lake.

where if a pixel was classified as water at least once, it was considered as a water pixel. Therefore, the total area of the masked area should be the same for different classification maps.

To better understand the spatial distributions of the transitions between different wetland features in Poyang Lake, three classification maps for 1973, 1995 and 2013 were used to generate the wetland transition maps in which the details of the two national reserves are also enlarged. Logically, 1973 and 2013 were chosen because they are placed at the start and end of the observed period, and the intermediate step has been fixed at 1995 because it roughly represents the mid-term year.

4. Results: Long-term wetland changes in Poyang Lake

After adjusting the surface reflectance to the same level as that of the OLI image in 2013, the 11 selected Landsat images were subsequently classified into four major wetland cover types (e.g., sand, water, vegetation, and mudflat), where the six-band classifier was used for the TM, ETM+, and OLI data, and the three-band SVM classifier was used for the left two MSS images.

Fig. 6 shows the classification maps for each of the Landsat images between 1973 and 2013. The spatial distributions of different wetland cover types were clearly demonstrated within each panel, and the long-term wetland changes were also revealed across each panel. In general, from the boundary to the center of Poyang Lake, the wetlands change from vegetation to mudflat and again to water body. The sand areas are relatively small for all of the maps, except for 1973. The wetland vegetation is primarily distributed in the southern and eastern regions of Poyang Lake, and these regions are where the two national reserves are located (see boundaries in Fig. 1). For the inundation area, a relatively large water body near the lake center close to Songmen Mountain could be easily identified from the Landsat observations between 1973 and 2002, but it was changed into other cover types (mainly mudflat) thereafter. In addition, wetland vegetation also shows significant variability, with generally larger areas observed after 2002.

To present the details of the major wetland changes in two national reserves, the classification maps in the two regions were enlarged and illustrated as shown in Figs. 7 and 8. Similar to the conditions of the

entire lake, the inundation area of the two national reserves rapidly decreased after 2002, and the sand areas were remained at a low level after 1984. In addition to the obviously expanded area, the wetland vegetation showed a trend spreading to the lake center in the NWNNR. As shown in the classified maps of 1973 and 1984, the wetland vegetation was primarily distributed along the southwest near-shore regions. However, a large area in the northeast NWNNR was covered by vegetation throughout the later years (especially after 2002). In contrast, after a rapid increase between 1973 and 1990, no significant variability was observed for the vegetation area of the PLNNR in terms of both spatial distribution and total area.

Fig. 9 plots the estimated areas of different wetland cover types (sand, vegetation and mudflat) between 1973 and 2013, where Fig. 9a, b, and c represent the results of the entire Poyang Lake, PLNNR, and NWNNR respectively. The coverage areas of wetland vegetation and mudflat fluctuated between 1973 and 2013. A statistically significant increasing trend ($p < 0.05$) was observed for vegetation area of the entire Poyang Lake during the four-decade period ($15.9 \text{ km}^2 \text{ year}^{-1}$) (note that $p < 0.05$ from the t-test was considered to be statistically significant in this study). At the same time, out-of-phase pattern was noted between the mudflat and wetland vegetation during the overall period. Specifically, the area of the mudflat showed a significant shrinking trend ($-12.1 \text{ km}^2 \text{ year}^{-1}$, $p < 0.05$) for the entire lake if the result in 1973 was not considered. Similar conditions were found in the NWNNR, where the wetland vegetation showed an increasing trend of $1.4 \text{ km}^2 \text{ year}^{-1}$ ($p < 0.05$) and the mudflat experienced a decreasing trend of $-1.3 \text{ km}^2 \text{ year}^{-1}$ ($p < 0.05$). In contrast, mudflat and vegetation in PLNNR did not change during the period observed. The sand area within the Poyang Lake boundary showed a remarkable decrease from 1973 to 1990 (from 544.3 km^2 to 62.9 km^2), which remained at a small coverage level ($<100 \text{ km}^2$) in the later period. The sand areas of the two national reserves changed in a manner similar to that of the entire lake.

The transition maps during the two periods of 1973–1995 and 1995–2013 are demonstrated in Fig. 10a and b, respectively. The dominant changes in the Poyang wetland in the first period (1973–1995) was that a large area of sand was transformed into vegetation

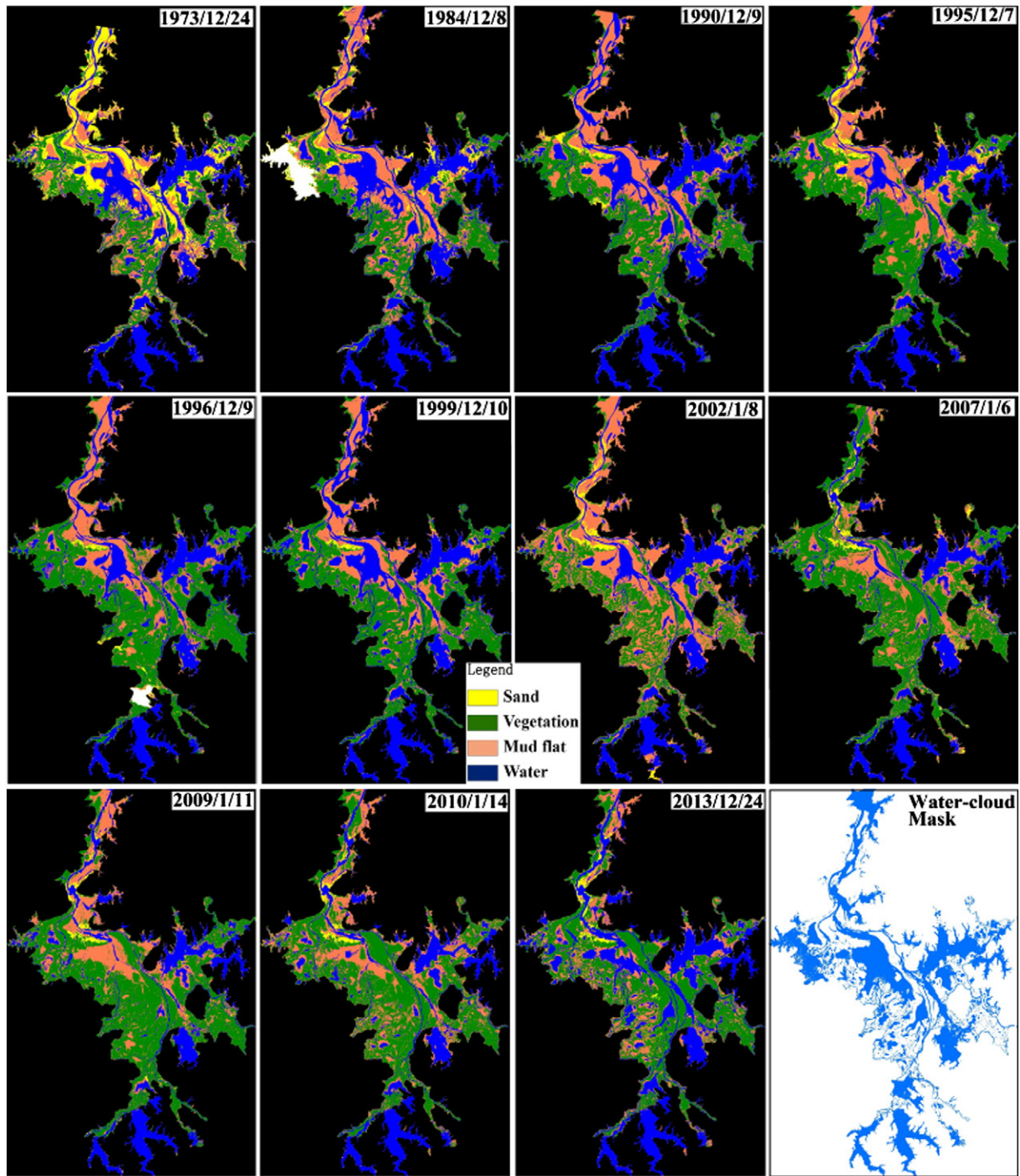


Fig. 6. Classification maps of Poyang Lake from four decades of Landsat observations between 1973 and 2013. The last panel shows the maximum inundation and cloud mask for further area statistics.

(195.0 km²) and mudflat (239.71 km²), and the changes were primarily distributed near the lake center. Additionally, a large area of mudflat (169.2 km²) was transitioned into wetland vegetation during this period, especially in the PLNNR. In contrast, the transitions from vegetation to mudflat or sand were negligible (<25 km²).

Significant land cover changes also occurred during the second period (1995–2013). Specifically, the coverage of sand within Poyang Lake was decreased because more sand was transitioned into wetland vegetation and mudflat than in the reverse directions. In addition, a large area of wetland vegetation was transformed into mudflat in the center lake regions. In the south area of Poyang Lake near the river mouth regions of Gan River and Xiu River, the wetland changes were

characterized by a transition from vegetation to mudflat. For the two national reserves, the dominant changes were also transformations between mudflat and vegetation.

5. Discussion

5.1. Driving forces

To test whether the growth of wetland vegetation was driven by air temperature, the relationship between the classified vegetation area in Poyang Lake and local temperature was examined. Correlation analysis showed a statistically significant correlation between the mean

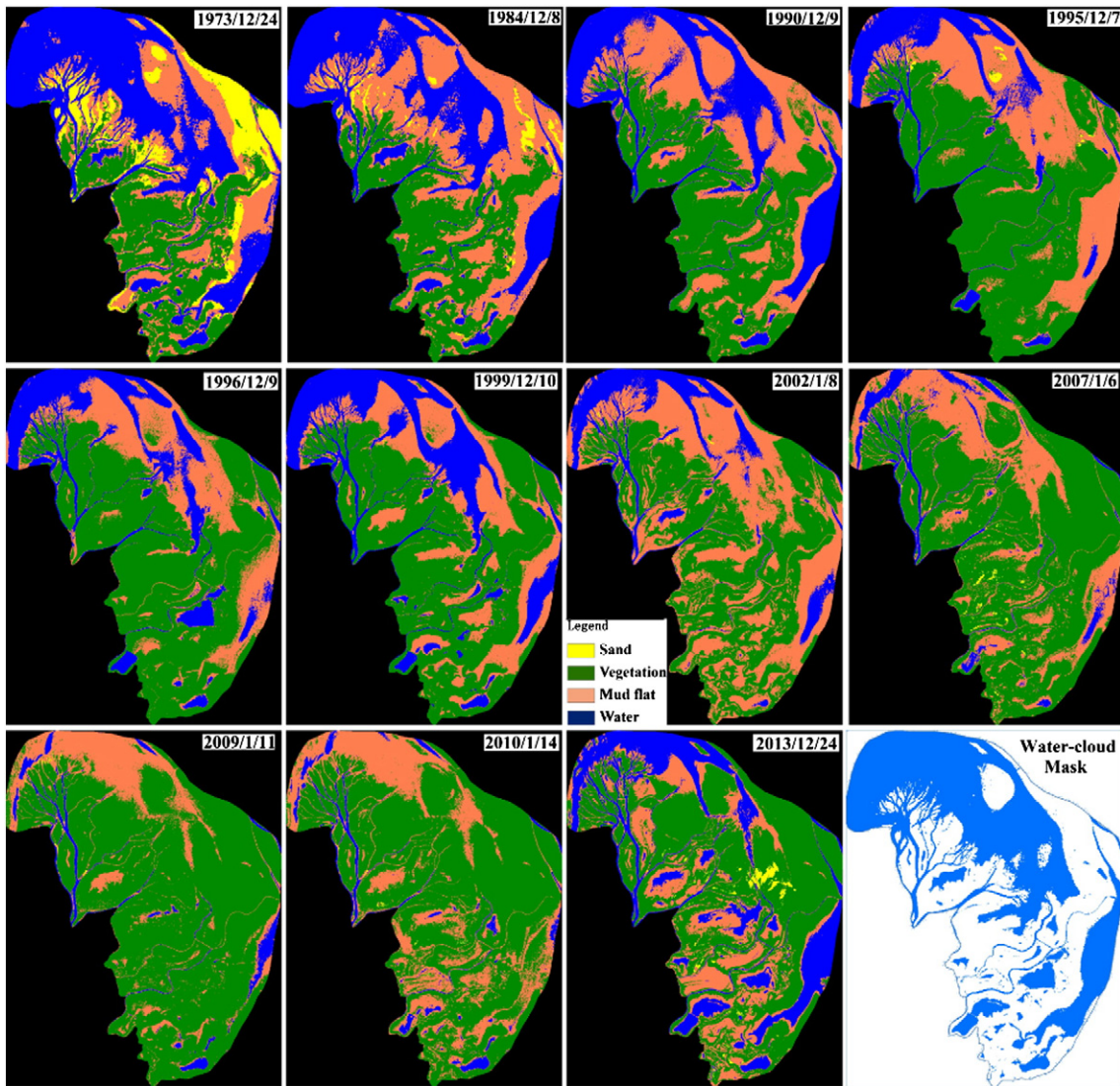


Fig. 7. Classification maps of NWNNR from four decades of Landsat observations between 1973 and 2013. The last panel shows the maximum inundation and cloud mask for further area statistics.

temperature from September to December and the vegetation area during each year, with a determination coefficient (R^2) of 0.72 for the entire Poyang Lake (see Fig. 11a), which is also statistically significant ($p < 0.05$, with t-test). Likewise, strong correlations were also found between temperature and vegetation area in the two national reserves (Fig. 11b and c). In other words, ~70% of the wetland vegetation variations in the dry seasons of Poyang Lake can be explained by local temperature during the last four decades.

The sediment input of the tributaries can change the turbidity of the lake water, thus regulating underwater light transmission and the growth of wetland vegetation (Erfemeijer & Robin Lewis Iii, 2006). Unfortunately, in plotting the Landsat derived vegetation area between 1990 and 2010 and the sediment flux in the wet season (April to September) (sediment data in other years are not available), no significant relationship was found between these factors over the entire lake (Fig. 12a) or the two national reserves (Fig. 12b, c). Additionally, changes in other meteorological and hydrological factors (i.e., precipitation and water level) might influence the biomass of the Poyang Lake region and thus the vegetation coverage. However, correlation studies between these environmental data and the vegetation area resulted in insignificant relationships, suggesting that the impact of these factors

on the vegetation growth is small over such a long period. Indeed, the occurrence of disturbances and other natural processes of change (i.e., ecological succession) could also lead to variability of the wetland vegetation, and their potential linkages could be studied once additional social and environmental data are available.

The sand area was considerably high at the beginning of the study period (1973), which subsequently transitioned into wetland vegetation and mudflat and remained at a low coverage level in the following years. The large sand coverage in 1973 could be linked to two important political campaigns in China between the 1950s and the 1970s, i.e., the Great Leap Forward Movement and the Great Cultural Revolution (Huang, 2005). Extreme behaviors occurred during these campaigns, i.e., intensive forest burning and cutting, leading to severe desertification and soil erosion in Poyang Lake and its drainage basin (Huang, 2005). Following these two campaigns, forest conservation and forestation efforts were encouraged by the local government, resulting in a restored ecosystem and decreased sand area in the later period.

The Three-Gorges Dam (TGD), the largest hydropower station in the world, was constructed in the upstream Yangtze River. It has been reported that the impoundment of the TGD in 2003 led to earlier dry-season starting dates in Poyang Lake for the post-TGD period (Feng,

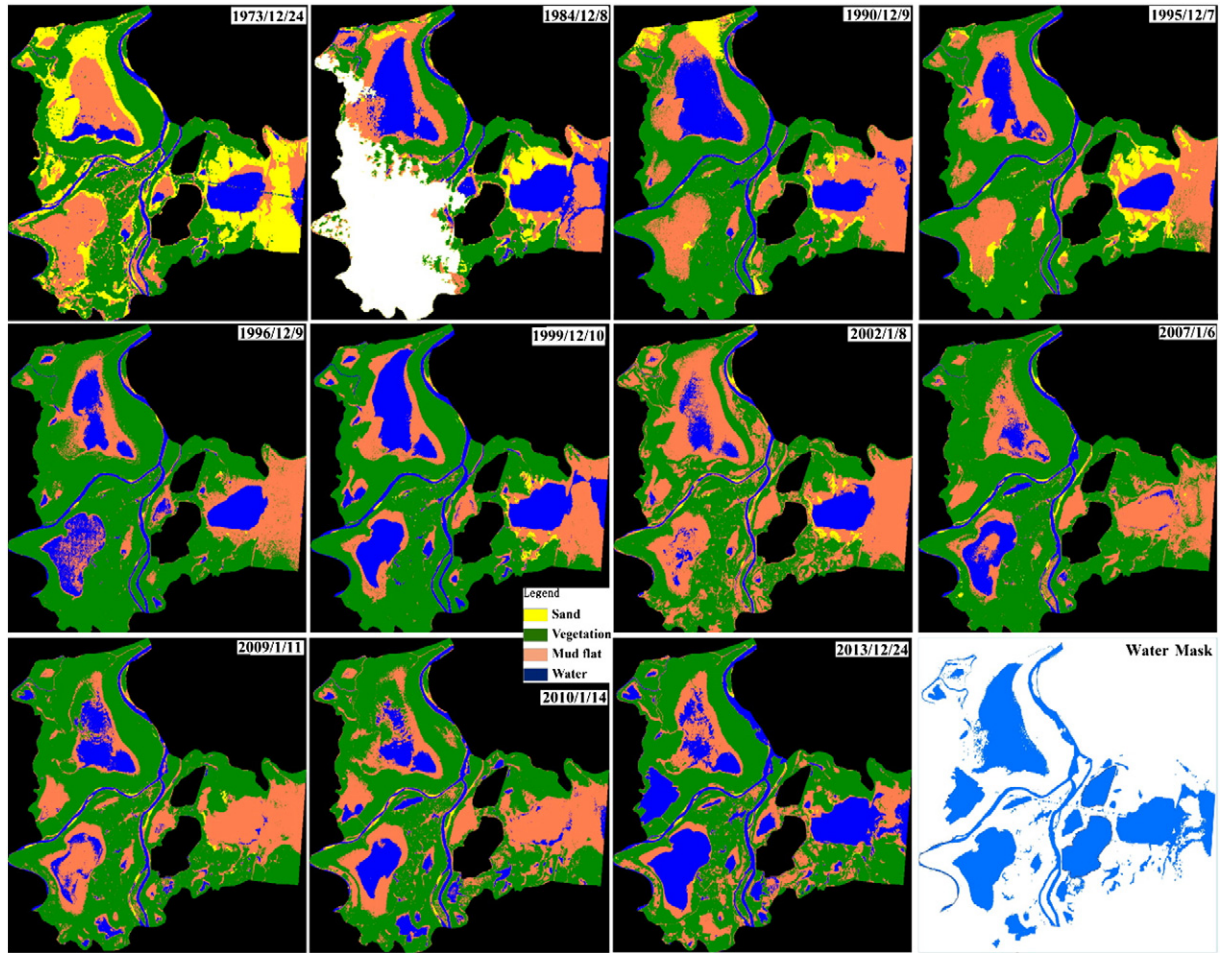


Fig. 8. Classification maps of PLNNR from four decades of Landsat observations between 1973 and 2013. The last panel shows the maximum inundation and cloud mask for further area statistics.

Hu, Chen, & Zhao, 2013). As a consequence, the exposure time of the lake bottom has been prolonged significantly, providing favorable conditions for vegetation growth within the lake boundary. Thus, the increase of vegetation area, especially after 2002, could possibly be due to the impoundment of the TGD, but the exact reason requires to be further investigation once additional hydrological and meteorological data are available.

5.2. Validity of the results

Long-term changes in major wetlands in Poyang Lake were clearly revealed and quantified for the first time via a rigorous analysis of Landsat observations. Due to the size and dynamic hydrological conditions, this historical information is difficult to obtain by other traditional methods (i.e., field surveys). However, are these remote-sensing based results valid?

The total signal received by the Landsat instruments contains radiance from both the target and the transmission path. Although a sophisticated atmospheric correction method was applied, residual errors might be remained in the surface reflectance (Kaufman et al., 1997). Fortunately, intense forest area is distributed near the Poyang Lake region, providing dark pixels and thus improving the accuracy of the atmospheric correction method (Kaufman et al., 1997). Moreover, the atmospheric correction errors could be compensated through empirical line correction because the reflectance of different images was adjusted to the same level as that of the OLI image in 2013. Therefore, the uncertainties of the surface reflectance to the classification maps should be small.

Landsat MSS is configured with four spectral bands over the visible-NIR region, but only three of them were analogous to subsequent Landsat instruments. However, the four wetland cover types in Poyang Lake show highly distinguishable spectral features in these spectral bands (see Fig. 3), allowing acceptable classification results with limited spectral information from Landsat MSS imagery. Indeed, the results demonstrated that classification maps produced with the three-band and six-band SVM methods are similar, the spatial distributions are nearly identical, and the difference between their overall accuracies is ~1.5%. Thus, the wetland classification obtained using different Landsat instruments were consistent in the overall period.

Ideally, the wetland of Poyang Lake should be studied with higher temporal resolution data than that of Landsat to account for the seasonality of different cover types. However, considering the high spatial resolution (30–60 m) and long data record (>40 years), Landsat appears to be the most suitable data for documenting the long-term wetland changes in Poyang Lake. For example, although two MODIS instruments provide daily global coverage, the 250-m resolution data appear to have difficulty in discriminating subtle wetland changes of Poyang Lake, especially in the two relatively small national reserves. In addition, MODIS data are only available since 2000, making it impossible to document the historical wetland conditions of several decades ago. Nevertheless, the Landsat images used in this study were collected between December and January of the next year, and the phenological and hydrological conditions of the Poyang Lake regions should be similar during each year. After masking the maximum inundation area, the classified wetland cover types within the lake boundary should be comparable across each year.

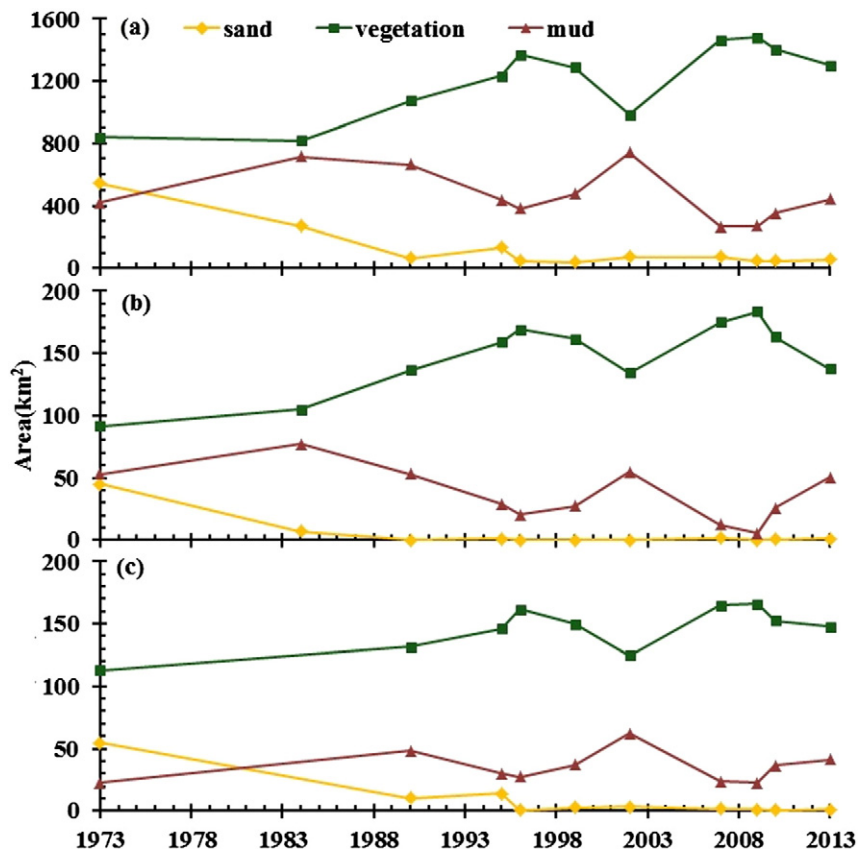


Fig. 9. (a) Long term changes of different wetland cover types in Poyang Lake during the overall period between 1973 and 2013. The conditions of NWNNR and PLNNR are also plotted in (b) and (c) respectively. Note that, the maximum surface area and clouds were masked prior to the area calculations.

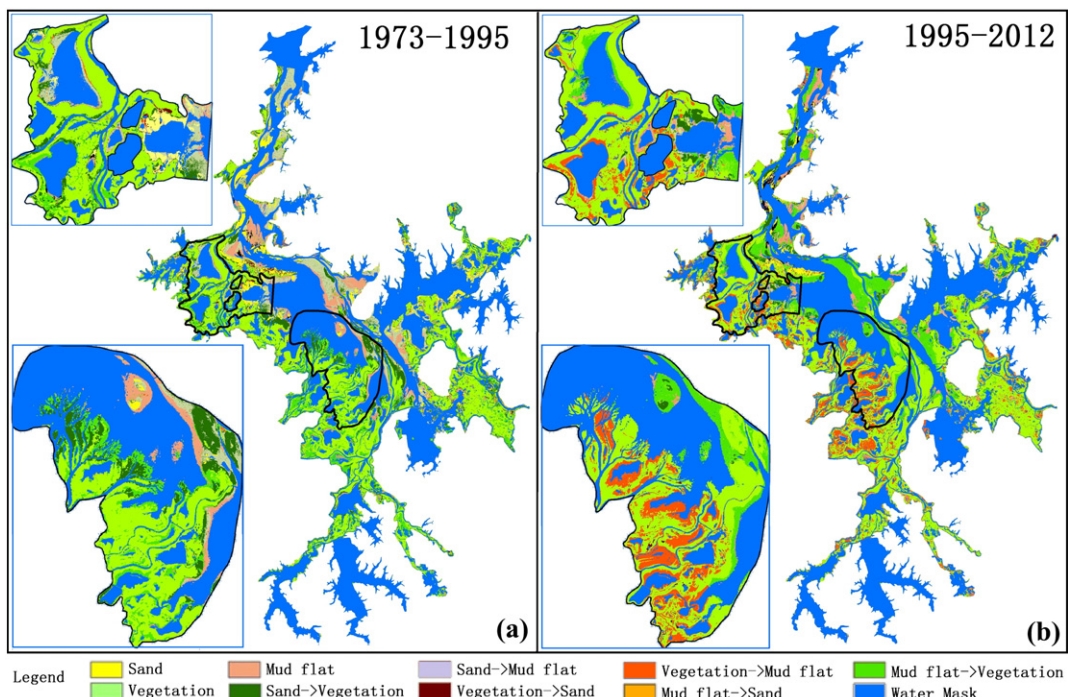


Fig. 10. The transition maps of different wetland cover types in Poyang Lake during two periods (1973–1995 and 1995–2012), where the two national reserves are enlarged to show their detailed changes.

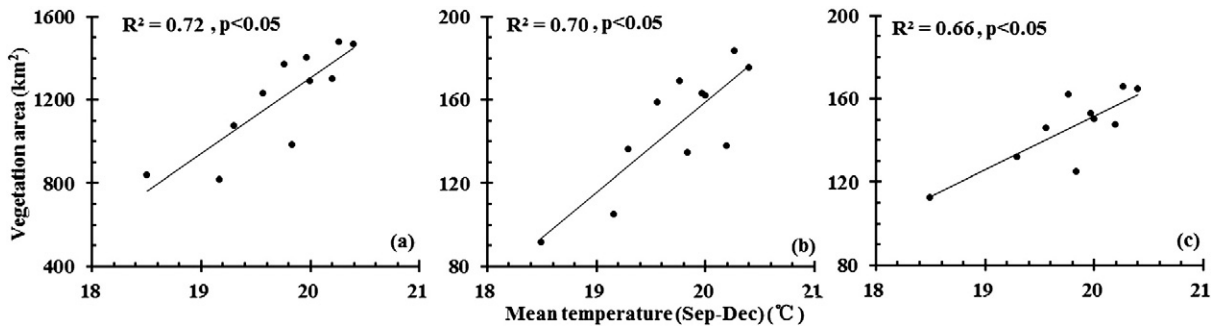


Fig. 11. Relationship between the vegetation area and mean temperature from September to December of that year. Significant correlations were found for the entire Poyang Lake (a) and two national reserves. (b) and (c) indicate NWNNR and PLNNR, respectively.

5.3. Implications and future applications

The findings of this study have significant implications in the long-term monitoring of the wetland ecosystems in Poyang Lake. Illegal sand dredging in the lake has led to rapid changes in water quality and lake morphology. For example, the total suspended sediment concentration of the north Poyang Lake increased from ~10 mg L⁻¹ in the early 2000s to >40 mg L⁻¹ in recent years, prohibiting light transmission in water and hence impacting the productivity of wetland vegetation, but the associated impact on the vegetation growth in that region could be assessed with the Landsat derived classification maps. In addition, in recognition of the frequently occurring drought in the Poyang Lake regions (Feng, Hu, Chen, Cai, et al., 2012), the local government has planned to build another dam in the lake to conserve its water storage. The classified wetland results in this work provide baseline information that could be used to optimize the operation of the future dam for conservation of wetland coverage in Poyang Lake.

From numerous field surveys conducted by the local environmental agencies and the work of our research group, we may reasonably conclude that the increased vegetation coverage in the close-water regions resulted from the flourishing growth of *C. cinerascens*, and as one of the most important wetland plant in Poyang Lake, its potential influence on the biodiversity and stability of the ecosystem in the Poyang Lake wetland could be assessed in the future with the assistance of the results in this study and other environmental and ecological knowledge.

The Chinese government has approved the implementation of high-definition earth observation system (HDEOS), and the first mission Gaofen-1 satellite (gaofen = high resolution), was successfully launched in 2013. With similar spectral bands and spatial resolution (Li, Feng, Pang, Zhao, & Gong, submitted for publication), the on-boarded high-frequency observations of WVF instruments are expected to provide better phenological information and species discrimination

(Wang et al., 2012), which are often more critical to study of the environmental sensitivity and ecological vulnerability of a wetland system.

6. Conclusions

Several findings were communicated in this study. The vegetation coverage of Poyang wetland showed a significant increasing trend during the overall study period, and the vegetation tended to spread into the lake center in the NWNNR. In contrast, a decreasing trend was observed for the mudflats. The coverage of vegetation and mudflats showed out-of-phase variability during the four-decade period. Rapid shrinkage of the sand area was detected from 1973 to 1990, after which the sand coverage remained relatively consistent in the Poyang Lake region. The mean temperature from September to December during each year was significantly correlated with the vegetation area within Poyang Lake, and the rapid increase after 2002 was possibly due to the impoundment of the TGD in 2003. The large sand area in 1973 could be linked to previous political campaigns of China between 1950s and 1970s.

To our knowledge, this is the first time that long-term changes in the major wetland cover types have been quantified in Poyang Lake. We attribute the success of this effort to the following factors: (1) access to over four decades of continuous global observations from Landsat series instruments, (2) an empirical line method applied to correct the differences between different sensors, (3) the robust method (SVM) used to obtain consistent classification results from remote sensing images collected by different instruments, and (4) the availability of various meteorological and ancillary data.

The results in this work provide baseline information for wetland changes in Poyang Lake, which could be used in the future for restoration purposes in the Poyang Lake ecosystem. In general, the approach

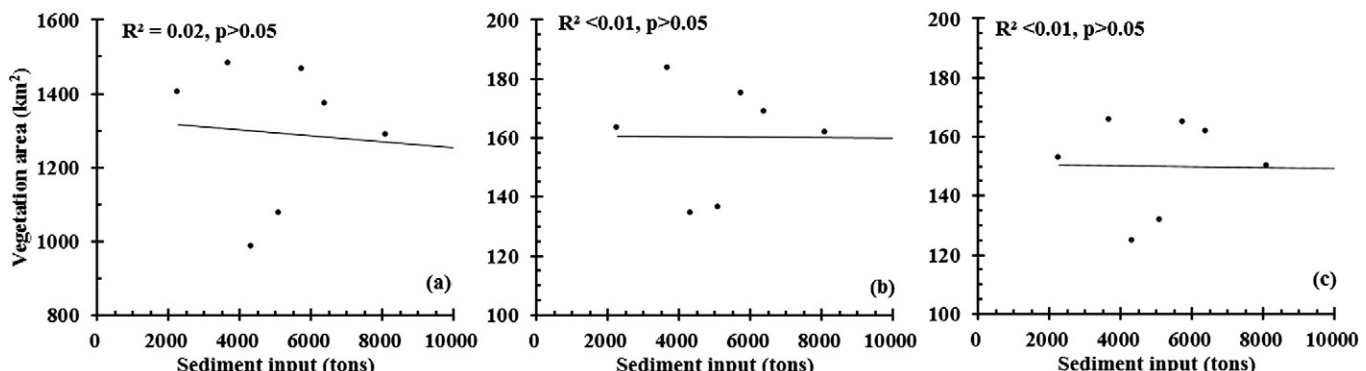


Fig. 12. Relationship between the vegetation area and sediment flux of the local tributaries of that year. No significant correlations were found for the entire Poyang Lake (a) and two national reserves. (b) and (c) indicate NWNNR and PLNNR, respectively.

demonstrated here could be easily extended to other similar wetlands to document and explore their changes over recent decades.

Acknowledgments

This work was supported by the National Natural Science Foundation of China (Nos. 41401388 and 41331174), the Fundamental Research Funds for the Central Universities, the Special Fund by Mapping Technology Plan in 2014 “Using UAV images to Identify and Extract Disaster Information” and the open-fund projects of LIESMARS (Wuhan University). We thank the USGS and the Remote Sensing Data Sharing Center of China for providing Landsat data. We are indebted to several local environmental agencies and groups who collected and provided meteorological and hydrological data. Two anonymous reviewers provided extensive comments that helped improve the manuscript.

References

- Adam, E., Mutanga, O., & Rugege, D. (2010). Multispectral and hyperspectral remote sensing for identification and mapping of wetland vegetation: A review. *Wetlands Ecology and Management*, 18, 281–296.
- Best, R., & Moore, D. (1979). Landsat interpretation of prairie lakes and wetlands of eastern South Dakota. *Proceedings Series-American Water Resources Association (USA)*.
- Chander, G., Markham, B.L., & Helder, D.L. (2009). Summary of current radiometric calibration coefficients for Landsat MSS, TM, ETM+, and EO-1 ALI sensors. *Remote Sensing of Environment*, 113, 893–903.
- Congalton, R.G. (1992). A review of assessing the accuracy of classifications of remotely sensed data. *Remote Sensing of Environment*, 37(1), 35–46.
- Dronova, I., Gong, P., Clinton, N.E., Wang, L., Fu, W., Qi, S., et al. (2012). Landscape analysis of wetland plant functional types: The effects of image segmentation scale, vegetation classes and classification methods. *Remote Sensing of Environment*, 127, 357–369.
- Dronova, I., Gong, P., & Wang, L. (2011). Object-based analysis and change detection of major wetland cover types and their classification uncertainty during the low water period at Poyang Lake, China. *Remote Sensing of Environment*, 115, 3220–3236.
- Erfemeijer, P.L.A., & Robin Lewis Iii, R.R. (2006). Environmental impacts of dredging on seagrasses: A review. *Marine Pollution Bulletin*, 52, 1553–1572.
- Feng, L., Hu, C., Chen, X., Cai, X., Tian, L., & Gan, W. (2012). Assessment of inundation changes of Poyang Lake using MODIS observations between 2000 and 2010. *Remote Sensing of Environment*, 121, 80–92.
- Feng, L., Hu, C., Chen, X., & Zhao, X. (2013). Dramatic inundation changes of China's two largest freshwater lakes linked to the Three Gorges Dam. *Environmental Science & Technology*, 47(17), 9628–9634.
- Finlayson, M., Harris, J., McCartney, M., Lew, Y., & Zhang, C. (2010). Report on Ramsar visit to Poyang Lake Ramsar site, P.R. China (pp. 1–34).
- Franklin, S., Gillespie, R., Titus, B., & Pike, D. (1994). Aerial and satellite sensor detection of *Kalmia angustifolia* at forest regeneration sites in central Newfoundland. *International Journal of Remote Sensing*, 15, 2553–2557.
- Gibbs, J.P. (2000). Wetland loss and biodiversity conservation. *Conservation Biology*, 14, 314–317.
- Gluck, M.J., Rempel, R.S., & Uhlig, P. (1996). An evaluation of remote sensing for regional wetland mapping applications. Sault Ste. Marie: Ontario Forest Research Institute.
- Gong, P., Niu, Z., Cheng, X., Zhao, K., Zhou, D., Guo, J., et al. (2010). China's wetland change (1990–2000) determined by remote sensing. *Science China Earth Sciences*, 53, 1036–1042.
- Green, E.P., Mumby, P.J., Edwards, A.J., Clark, C.D., & Ellis, A.C. (1997). Estimating leaf area index of mangroves from satellite data. *Aquatic Botany*, 58, 11–19.
- Hines, M.E., Pelletier, R.E., & Crill, P.M. (1984–2012). Emissions of sulfur gases from marine and freshwater wetlands of the Florida Everglades: Rates and extrapolation using remote sensing. *Journal of Geophysical Research, [Atmospheres]*, 98, 8991–8999.
- Hinson, J.M., German, C.D., & Pulich, W., Jr. (1994). Accuracy assessment and validation of classified satellite imagery of Texas coastal wetlands. *Marine Technology Society Journal*, 28, 4–9.
- Houlihan, J.E., Keddy, P.A., Makkay, K., & Findlay, C.S. (2006). The effects of adjacent land use on wetland species richness and community composition. *Wetlands*, 26, 79–96.
- Huang, G. (2005). Ecological and environment problems of Jiangxi Province and its impact on GDP. *Proceedings of China's sustainable development forum in 2005. Shanghai, China*.
- Jensen, J.R. (1996). *Introductory digital image processing: A remote sensing perspective*. Prentice-Hall Inc.
- Johnston, R.M., & Barson, M.M. (1993). Remote sensing of Australian wetlands: An evaluation of Landsat TM data for inventory and classification. *Marine and Freshwater Research*, 44, 235–252.
- Kanai, Y., Ueta, M., Germogenov, N., Nagendran, M., Mita, N., & Higuchi, H. (2002). Migration routes and important resting areas of Siberian cranes (*Grus leucogeranus*) between northeastern Siberia and China as revealed by satellite tracking. *Biological Conservation*, 106, 339–346.
- Kaufman, Y., Tanré, D., Remer, L.A., Vermote, E., Chu, A., & Holben, B. (1997). Operational remote sensing of tropospheric aerosol over land from EOS moderate resolution imaging spectroradiometer. *Journal of Geophysical Research, [Atmospheres]*, 102, 17051–17067.
- Keddy, P.A. (2010). *Wetland ecology: Principles and conservation*. Cambridge University Press.
- Kempka, R., Kollasch, R., & Koeln, G. (1992). Ducks unlimited: Using GIS to preserve the Pacific Flyway's wetland resource. *GIS World*, 5, 46–52.
- Knorr, J., Rabe, A., Radloff, V.C., Kuemmerle, T., Kozak, J., & Hostert, P. (2009). Land cover mapping of large areas using chain classification of neighboring Landsat satellite images. *Remote Sensing of Environment*, 113, 957–964.
- Kovacs, J.M., Flores-Verdugo, F., Wang, J., & Aspden, L.P. (2004). Estimating leaf area index of a degraded mangrove forest using high spatial resolution satellite data. *Aquatic Botany*, 80, 13–22.
- Kovacs, J.M., Wang, J., & Flores-Verdugo, F. (2005). Mapping mangrove leaf area index at the species level using IKONOS and LAI-2000 sensors for the Agua Brava Lagoon, Mexican Pacific. *Estuarine, Coastal and Shelf Science*, 62, 377–384.
- Lee, C.T., & Marsh, S.E. (1995). The use of archival Landsat MSS and ancillary data in a GIS environment to map historical change in an urban riparian habitat. *Photogrammetric Engineering and Remote Sensing*, 61, 999–1008.
- Li, T. (2008). Crisis at Poyang Lake. *China dialogue*.
- Li, J., Feng, L., Pang, X., Zhao, X., & Gong, J. (2014n). A novel method to calibrate Gaofen-1 WV cameras using concurrent Landsat-8 OLI images. *IEEE Transactions on Geoscience and Remote Sensing* (submitted for publication).
- Luczkovich, J., Wagner, T., Michalek, J., & Stoffle, R. (1993). Discrimination of coral reefs, seagrass meadows, and sand bottom types from space: A Dominican Republic case study. *Photogrammetric Engineering and Remote Sensing*, 59, 385–389.
- Macleod, R.D., & Congalton, R.G. (1998). A quantitative comparison of change-detection algorithms for monitoring eelgrass from remotely sensed data. *Photogrammetric Engineering and Remote Sensing*, 64, 207–216.
- Margono, B.A., Bwangoy, J.-R.B., Potapov, P.V., & Hansen, M.C. (2014). Mapping wetlands in Indonesia using Landsat and PALSAR data-sets and derived topographical indices. *Geo-spatial Information Science*, 17(1), 60–71.
- Mitsch, W.J., & Gosselink, J.G. (2000). The value of wetlands: Importance of scale and landscape setting. *Ecological Economics*, 35, 25–33.
- Ozesmi, S.L., & Bauer, M.E. (2002). Satellite remote sensing of wetlands. *Wetlands Ecology and Management*, 10, 381–402.
- Poirson, C., Couteron, P., & Fromard, F. (2007). Predicting and mapping mangrove biomass from canopy grain analysis using Fourier-based textural ordination of IKONOS images. *Remote Sensing of Environment*, 109, 379–392.
- Shankman, D., Keim, B.D., & Song, J. (2006). Flood frequency in China's Poyang Lake region: Trends and teleconnections. *International Journal of Climatology*, 26, 1255–1266.
- Smith, G.M., & Milton, E.J. (1999). The use of the empirical line method to calibrate remotely sensed data to reflectance. *International Journal of Remote Sensing*, 20, 2653–2662.
- Tan, Q., Shao, Y., Yang, S., & Wei, Q. (2003). Wetland vegetation biomass estimation using Landsat-7 ETM+ data. *Geoscience and Remote Sensing Symposium, 2003. IGARSS'03. Proceedings. 2003 IEEE International* (pp. 2629–2631). IEEE.
- Wang, L., Dronova, I., Gong, P., Yang, W., Li, Y., & Liu, Q. (2012). A new time series vegetation–water index of phenological–hydrological trait across species and functional types for Poyang Lake wetland ecosystem. *Remote Sensing of Environment*, 125, 49–63.
- Wu, G., Leeuw, J. d., Skidmore, A.K., Prins, H.H.T., & Liu, Y. (2005). Exploring the possibility of estimating the aboveground biomass of *Vallisneria spiralis* L. using Landsat TM image in Dahuchi, Jiangxi Province, China. *Proc. SPIE 6045, 60452P*.
- Zhang, B. (Ed.). (1988). *Research of Poyang Lake*. Shanghai: Shanghai scientific & Technical Publishers.